Virologica Sinica 37 (2022) 664–675

Contents lists available at ScienceDirect

Virologica Sinica

journal homepage: www.keaipublishing.com/en/journals/virologica-sinica
www.virosin.org

Research Article

Transmembrane domain of IFITM3 is responsible for its interaction with influenza virus HA_2 subunit

Wang Xu [a], Yuhang Wang [b], Letian Li [c], Xiaoyun Qu [d], Quan Liu [d], Tiyuan Li [b], Shipin Wu [b], Ming Liao [d], Ningyi Jin [a,c,*], Shouwen Du [b,*], Chang Li [c,*]

[a] College of Veterinary Medicine, Northwest A&F University, Yangling, 712100, China
[b] Department of Infectious Diseases, The Second Clinical Medical College of Jinan University, Shenzhen, 518020, China
[c] Research Unit of Key Technologies for Prevention and Control of Virus Zoonoses, Chinese Academy of Medical Sciences, Changchun Veterinary Research Institute, Chinese Academy of Agricultural Sciences, Changchun, 130122, China
[d] Key Laboratory of Zoonosis of Ministry of Agriculture, South China Agricultural University, Guangzhou, 510642, China

ARTICLE INFO

Keywords:
Interferon-inducible transmembrane protein 3 (IFITM3)
Influenza virus
Hemagglutinin (HA)
Interaction
Transmembrane domain

ABSTRACT

Interferon-inducible transmembrane protein 3 (IFITM3) inhibits influenza virus infection by blocking viral membrane fusion, but the exact mechanism remains elusive. Here, we investigated the function and key region of IFITM3 in blocking influenza virus entry mediated by hemagglutinin (HA). The restriction of IFITM3 on HA-mediated viral entry was confirmed by pseudovirus harboring HA protein from H5 and H7 influenza viruses. Subcellular co-localization and immunocoprecipitation analyses revealed that IFITM3 partially co-located with the full-length HA protein and could directly interact with HA_2 subunit but not HA_1 subunit of H5 and H7 virus. Truncated analyses showed that the transmembrane domain of the IFITM3 and HA_2 subunit might play an important role in their interaction. Finally, this interaction of IFITM3 was also verified with HA_2 subunits from other subtypes of influenza A virus and influenza B virus. Overall, our data demonstrate for the first time a direct interaction between IFITM3 and influenza HA protein via the transmembrane domain, providing a new perspective for further exploring the biological significance of IFITM3 restriction on influenza virus infection or HA-mediated antagonism or escape.

1. Introduction

Interferon-inducible transmembrane (IFITM) proteins are a family of small transmembrane proteins that localize in the plasma and endolysosomal membranes and inhibit viral infections by impeding virus entry and reducing the production of infectious virions (Yánez et al., 2020; Marziali and Cimarelli, 2021; Majdoul and Compton, 2022). Among them, IFITM3 is a conserved cellular transmembrane protein (133 amino acids) which resides in late endosomes and lysosomes and inhibits fusion of various enveloped viruses by blocking formation of fusion pores at the post-hemifusion stage (Coomer et al., 2021; Majdoul and Compton, 2022). Based on the proximity principle of IFITM3 inhibition (Suddala et al., 2019), the possible mechanisms of IFITM3 that block the viral membrane fusion include: firstly, IFITM3 might establish a barrier "hand in hand" to block the entry of the virus (Winkler et al., 2019); secondly, IFITM3 can incorporate into the nascent viral particles (Compton et al., 2014; Spence et al., 2019), which results in weakened viral infection, but this remains controversial or divisive (Foster et al., 2016); thirdly, IFITM3 limits viral fusion by affecting the membrane fluidity and/or cholesterol transport or biosynthesis (Amini-Bavil-Olyaee et al., 2013; Lin et al., 2013; Nm et al., 2017), but this also remains controversial. Even vesicle-associated membrane protein-associated protein A (VAPA) has shown direct interaction with IFITM3, which is difficult to reveal the mechanism of its antiviral activity (Amini-Bavil-Olyaee et al., 2013).

Currently, there are four influenza types in nature, influenza viruses A to D, among which influenza A virus (IAV) is the most virulent pathogen, causing severe disease in humans, domestic poultries, birds, and animals. IAVs have evolved into several serotypes based on the surface glycoproteins (hemagglutinin, HA) and neuraminidase (NA) (Hay et al., 2001; Tong et al., 2013). HA protein is the receptor-binding glycoprotein and exists on the surface of virus particles as trimer. HA protein consists of HA_1 and HA_2 subunits. The virus-membrane-distal HA_1 head is responsible for receptor binding and HA_2 subunit anchors to the viral membrane to be responsible for the fusion of the viral envelope with the endosomal

* Corresponding authors.
E-mail addresses: ningyik@126.com (N. Jin), du-guhong@163.com (S. Du), lichang78@163.com (C. Li).

https://doi.org/10.1016/j.virs.2022.07.002
Received 6 April 2022; Accepted 30 June 2022
Available online 6 July 2022

membrane (Wagner et al., 2002; Nayak et al., 2004; Floyd et al., 2008; Hamilton et al., 2012; Boonstra et al., 2018). However, the molecular mechanism and action mode of IFITM3 to prevent viral fusion mediated by HA protein are not yet clear.

At present, the importance of the IFITM3-mediated inhibition of IAV infection *in vitro* and *in vivo* has been demonstrated through the association of its polymorphism with the severity of IAV disease in human infection (Everitt et al., 2012; Wellington et al., 2019; Ren et al., 2020) and the relevance of *Ifitm3* knockout with the increased the morbidity and mortality in mice infection (Bailey C.C. et al., 2012; Kenney et al., 2019; Sun Q. et al., 2020). Nonetheless, the molecular mechanism of IFITM3 restricts viral fusion is still under investigation. Recent study have shown that the incorporation of IFITM3 into influenza virus particles reduces the HA protein on virus particle surface, making the virus more sensitive to neutralizing antibodies (Lanz et al., 2021). IAV infection induces IFITM3 clustering and localization to endosomal vesicles in primary human airway epithelial cells not just an increase in its abundance, resulting into the formation of IFITM3-coated and IAV-carrying vesicles, to efficiently block IAV infection (Kummer et al., 2019; Suddala et al., 2019). These studies support the notion that IFITM3 oligomers inhibit viral-cell fusion by IFITM3-IFITM3 interaction or promoting membrane rigidity (Winkler et al., 2019; Rahman et al., 2020; Guo et al., 2021). And zoonotic H5N1 and H7N9 viruses escape IFITM3 restriction with a relatively high pH optimum of fusion in endothelial cells, providing a correlation between the IFITM3 inhibition and HA stability (Hensen et al., 2019). In addition, post-translational modifications of the conserved residues and some important motifs on IFITM3 such as N-terminal YEML motif, a GxxxG motif, the conserved cysteine residues, F75 and F78, are the prerequisites for its antiviral activity (Chesarino N.M. et al., 2017; Mcmichael et al., 2017; Huang D. L. et al., 2020; Rahman et al., 2020).

In this study, the mechanism of IFITM3 restriction on HA-mediated viral entry was further explored. Also, whether IFITM3 had direct interaction with HA proteins derived from representative isolates of different serotypes was investigated. The HA subunit and domains, which involved in IFITM3-mediated restriction of influenza virus were further determined. The key domain of IFITM3 interacts with the HA was also verified. In addition, the interaction between IFITM3 and other subtypes of influenza was also investigated. Our data provide important insights into the function of IFITM3 against influenza infection.

2. Materials and methods

2.1. Cells

HEK293 (GNHu 43), HEK293T (SCSP-502), HeLa (TCHu187) and MDCK (ATCC: CCL-34) cells were grown in Dulbecco's modified Eagle's medium (DMEM) supplemented with 10% heat-inactivated fetal bovine serum. A549 cells (SCSP-503) were maintained in Ham's F-12K (Kaighn's) medium (Gibco, USA) supplemented with 10% fetal bovine serum (FBS; Gibco, USA) and 1% penicillin-streptomycin (Solarbio, China), and used to generate the IFITM3-knockdown cells by the targeting short hairpin RNA (shRNA). HEK293, HEK293T, HeLa and A549 cells were donated by Stem Cell Bank, the Chinese Academy of Sciences. MDCK cells were kindly donated by Professor Ningyi Jin. The inducible IFITM3-expressing MDCK and HEK293 cells (MDCK-Tet3G-IFITM3 and HEK293-Tet3G-IFITM3) were generated based on the Tet-On3G system as described previously (Cao et al., 2017).

2.2. Plasmid construction

For preparing the HA-pseudotyped virus, the full-length *HA* gene fragments were amplified from the viral cDNA of avian influenza virus H5N1 (A/chicken/Jilin/9/2004 strain) and influenza virus H7N9 (A/Shanghai/4664T/2013) and then inserted into the eukaryotic expression vector pcDNA3.1 (+) (ThermoFisher Scientific, USA).

For intracellular localization and interaction analysis, the human *IFITM3* gene and its truncated domains NTD, IMD-CIL, and CIL-TMD that were fused with EGFP at the C-terminus were cloned into the pEGFP-N1 vector, and the *IFITM3* that was fused with either mCherry or Flag tag at the C-terminus was cloned into the pmCherry-N1 or pVAX1 vector. The full-length *HA* (*H5* and *H7*) gene and their truncated fragments encoding HA_1 ($H5_1$ and $H7_1$) subunits fused with an EGFP at the C-terminus were cloned into the pEGFP-N1 vector. Also, the *HA* gene fragments encoding HA_2 ($H5_2$ and $H7_2$) subunits and the truncated domains ΔFP_HA_2 (lacking the fusion peptide), ΔTM_HA_2 (without the transmembrane domain), and stalk region (including a three-fold axis without FP and TM domains) fused with a mCherry tag at the C-terminus were constructed based on the pmCherry-N1 vector. All plasmids were verified by DNA sequencing.

2.3. Pseudotyped virus production and infection

To generate influenza A virus HA pseudotyped virus, HEK293T cells were transfected with a three-plasmid mix of the luciferase reporter vector pLentiCMV-Luc2, pCMV-dR8.2-dvpr packaging vector, and pcDNA3.1-H5 or H7 encoding influenza virus envelope glycoproteins or VSV-G protein expression plasmid to produce pseudotype viruses. According to the protocol, the pseudoviruses were then harvested for 48 h after transfection and titrated with the Lenti-X qRT-PCR Titration Kit (Takara, Japan). For HA-pseudotyped virus entry assays, Dox or DMSO pre-treated MDCK- or HEK293-Tet3G-IFITM3 cells were infected with the pseudoviruses (MOI = 1.0) for 48 h and then were washed and lysed for detecting luciferase signal (relative luciferase units or RLU) with ONE-Glo™ luciferase assay system (Promega, USA) according to the instructions.

2.4. Membrane Protein Isolation

The plasma membrane protein was isolated using the Minute Plasma Membrane Isolation kit according to the manufacture's instructions (Invent Biotechnologies, USA). In brief, the cells were collected and resuspended with lysis buffer A supplemented with Complete™ EDTA-free Protease Inhibitor Cocktail (Roche, #4693116001, Switzerland). The total membrane proteins, including organelles and plasma membrane, were isolated by centrifugation and further analyzed by Western blotting with the indicated antibodies.

2.5. Western blotting

The PBS-washed cells were lysed by Cell lysis buffer (Beyotime, China) with 1% Complete™ EDTA-free protease inhibitor cocktail (Roche, #4693116001, Switzerland) and 1 mmol/L PMSF (Beyotime, China) on ice for 15 min. A certain amount of cell lysates was separated by SDS-polyacrylamide gel electrophoresis and then transferred onto nitrocellulose membranes (Millipore, Germany). The membranes were probed with appropriate primary antibodies and horseradish peroxidase-conjugated goat anti-rabbit or mouse IgG (Beyotime, China). The protein bands were detected by Western blotting HPR substrate (Millipore, Germany) using the FluorChem imagers (Protein-simple, USA).

The primary antibodies used in this study include Rabbit polyclonal anti-IFITM3 (Proteintech, Cat# 11714-1-AP, USA), FLAG-tag Polyclonal Antibody (MultiSciences, Cat# ab30107, China), β-Actin Mouse mAb (MultiSciences, Cat# ab008, China), Anti-HA (H5N1) (Avian) (Immune Technology, Cat# IT-003-006, USA), Anti-HA (H7N9) (A/Shanghai/1/2013) (Immune Technology, Cat# IT-003-0073M1, USA), Anti-EGFP antibody (F56-6A1.2.3) (Abcam, Cat# ab184601, UK), Anti-mCherry antibody (Abcam, Cat# ab167453, UK), GAPDH (14C10) Rabbit mAb (Cell Signaling Technology, Cat# 2118, USA), and Myc-tag Polyclonal Antibody (MultiSciences, Cat# ab30104, China). The secondary antibodies used in this study include Goat Anti-Rabbit IgG (HRP) (Beyotime,

Cat# A0208, China) and Goat Anti-Rabbit IgG (HRP) (Beyotime, Cat# A0216, China).

2.6. Co-immunoprecipitation (Co-IP)

For co-immunoprecipitation, the HEK293T cells were co-transfected with two expression plasmids of EGFP-fused protein and mCherry-fused protein or Flag-fused protein for 48 h. The cells were collected and washed twice with cold 1 × PBS and then lysed in the IP lysis buffer (Beyotime, China) for 30 min on ice. The lytic supernatants were incubated with agarose beads by covalently coupling to anti-EGFP or anti-mCherry Alpaca single-molecule nanoantibodies (AlpaLife, China) overnight at 4 °C to isolate the immune complexes. The beads were then washed thrice with cold lysis buffer before immunoprecipitation complexes were resuspended with 1 × SDS loading buffer, separated by SDS-PAGE, and then immunoblotted with specific antibodies.

2.7. Confocal microscopy

The cells were cultured on glass coverslips (Solarbio, China) for the indicated treatment concentrations, then fixed in 4% paraformaldehyde and PBS for 30 min, and then permeabilized with 0.25% Triton X-100 according to the specific requirement. The nuclei were stained with DAPI (Invitrogen, USA). The images were taken under a fluorescence microscope or the Leica TCS SP8 confocal microscope.

2.8. Statistics and reproducibility

All experiments were repeated at least three times unless otherwise stated. The data were presented as means ± standard deviation (SD). Statistical analyses were performed using the SPSS 13.0 and GraphPad Prism 9 software. All presented micrographs are representative images of three representative experiments as indicated in the Fig legends. For quantitative data of the indicated experiments, the *P*-values between the two groups were determined using an unpaired *t*-test. Furthermore, one-way ANOVA was used for results encompassing multiple groups. The *P* values of less than 0.05 between the two groups were considered significant.

3. Results

3.1. Hemagglutinin-mediated viral entry is restricted by IFITM3

HA acts as a homotrimer when present on the viral surface that undergoes a conformational change in the low pH environment of the endosome, resulting in the exposure to fusion peptides to trigger the fusion of the viral envelope and endosomal membrane (Floyd et al., 2008; Boonstra et al., 2018). In this process, IFITM3 functions as a restriction (Suddala et al., 2019), but the mechanism remains unclear. To confirm whether HA-mediated viral entry was restricted by IFITM3, IFITM3-knockdown A549, IFITM3-overexpressing MDCK or HEK293 cell lines were infected with H5 or H7 pseudotyped viruses, respectively. As shown in Fig. 1A, knockdown of IFITM3 markedly increased H5-mediated virus entry in pseudoviruses infection. And, infection analysis of H5 or H7 pseudotyped viruses showed that when compared with DMSO treated cells, luciferase production was inhibited in Dox-induced IFITM3 expression cells (Fig. 1B and C), indicating that the induced IFITM3 inhibited the HA-mediated viral entry in MDCK or HEK293 cells.

3.2. IFITM3 partially co-locates with full-length HA and binds HA conditionally

Previous study showed that IFITM3 hinders fusion pore formation (Desai et al., 2014). However, whether IFITM3 can interact with HA protein was unknown. The recombinant plasmids encoding IFITM3 tagged with C-terminal mCherry (IFITM3-mCherry) and EGFP-fused HA in C-terminal (H5-EGFP and H7-EGFP) were constructed to investigate the co-localization and interaction of IFITM3 and HA using laser confocal microscope and immunoprecipitation analysis. Co-localization analysis revealed that the fluorescently labeled IFITM3 showed partial co-location with HA in HEK293T cells (Fig. 1D). In addition, the immunoblotting analysis showed that in contrast with a single and complete band of H7-EGFP, H5 fused with EGFP might be cleaved by post-translation in HEK293T cells (Fig. 1E), and this was probably related to the strength of the proteolytic cleavage sites (Russell et al., 2018). The interaction of IFITM3 and HA was further investigated via immunoprecipitation analysis based on the co-expression of IFITM3-mCherry with H5-EGFP or H7-EGFP in cells. The results showed that IFITM3-mCherry could capture H5-EGFP but not H7-EGFP by anti-mCherry antibody-bound beads (Fig. 1F and G). Altogether, our results demonstrate that IFITM3 partially co-locates with full-length HA and binds HA conditionally in case of exogenous expression, which may be related to HA cleavage strength.

3.3. IFITM3 interacts with HA2 subunit of H5 and H7 subtypes

The HA_0 protein undergoes post-translation modification during the virus replication cycle for cleaving into two distinct subunits, HA_1 and HA_2 (Fig. 2A), linked by disulfide bonds (Russell et al., 2018). On the surface of influenza viral particles, HA protein exists in a metastable state, forming a homotrimer of disulfide-linked heterodimers that was composed of the receptor-binding subunit (HA_1) and the membrane fusion subunit (HA_2) (Fig. 2B). In the late endosomes, the HA protein undergoes conformational changes, resulting in the exposure of fusion peptides near the N-terminus of HA_2, which will then be inserted into the endosomal membrane and interact with the transmembrane domain near the C-terminus of HA_2 to facilitate pore formation (Lai and Freed, 2015; Chang et al., 2008). Therefore, we speculated a possibility of interaction between IFITM3 and HA_2 subunits. To further investigate our hypothesis, the recombinant expression plasmids encoding Flag-tagged IFITM3 (IFITM3-Flag), EGFP-fused HA_1 ($H5_1$-EGFP and $H7_1$-EGFP), or mCherry-fused HA_2 ($H5_2$-mCherry and $H7_2$-mCherry) were first constructed and identified to express the corresponding target protein. The location analysis in HeLa cells showed that fluorescent probe fused $H5_2$ or $H7_2$ subunit was co-localized with Rab7 and LAMP1, almost completely co-localized with LAMP1 (Fig. 2C), indicating that the exogenous expressed $H5_2$ and $H7_2$ subunits are located mainly in the late endosomal and lysosomal compartments. Moreover, the localization analysis of IFITM3-EGFP and $H5_2$-mCherry or $H7_2$-mCherry proteins showed that the IFITM3 was co-localized with the $H5_2$ or $H7_2$ subunit (Fig. 3A).

Next, to evaluate whether direct interaction occurs between IFITM3 and HA_2 subunit, the membrane protein mixture of IFITM3-EGFP and $H5_2$-mCherry or $H7_2$-mCherry was isolated for immunoprecipitation with an anti-EGFP tag to avoid the interference of other cytoplasmic proteins (Fig. 3B). Despite some uncertain protein interference, IFITM3 could capture $H5_2$ or $H7_2$ subunit in the membrane protein extracts (Fig. 3C). In contrast, co-immunoprecipitation analysis of IFITM3-Flag with $H5_1$ or $H7_1$-EGFP revealed that $H5_1$ or $H7_1$ could not capture IFITM3 protein via anti-EGFP tag, demonstrating no direct interaction between IFITM3 and HA_1 subunit (Fig. 3D). Together, the above results supported that IFITM3 interacts with the HA_2 subunit of HA, which might be a novel mechanism of IFITM3 restriction to viral membrane fusion.

3.4. The interaction between IFITM3 and HA_2 subunit is mediated by binding to the transmembrane region of HA

HA_2 subunit consists of FP, Hairpin 1 (Hp-1), helix A (H-A), Loop B (L-B), helix C (H–C), and helix D (H-D), Hairpin 2 (Hp-2), TMD and C-terminal (Fig. 2A) (Skehel and Wiley, 2000). To determine which domain of the HA_2 subunit was responsible for interacting with IFITM3, the HA_2 chain was then fragmented and cloned into the expression vector

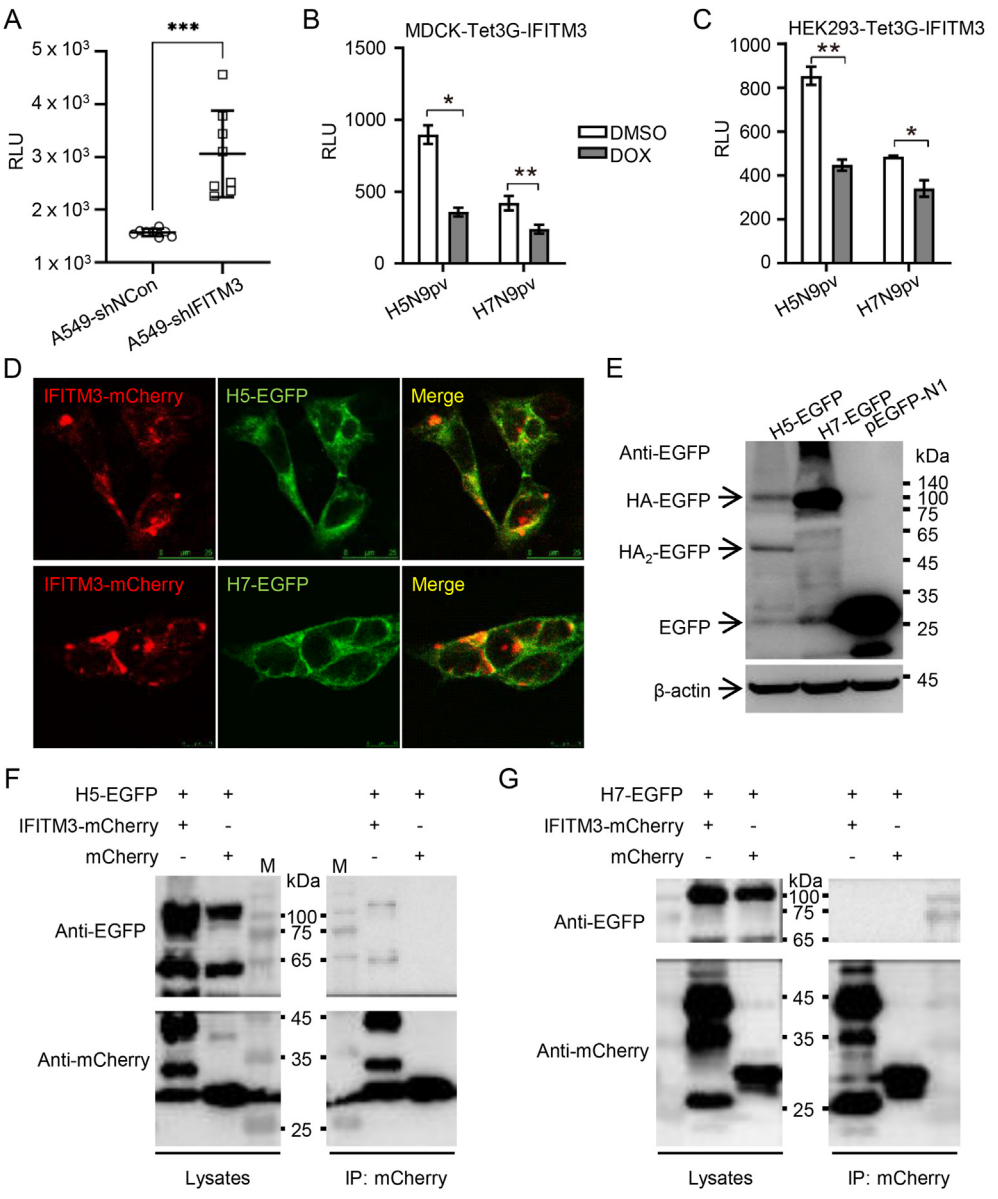

Fig. 1. Sensitivity of HA-pseudotyped viruses to IFITM3. **A** Quantitation of H5-pseudoviruses infection by determining luciferase activity in cell lysates. A549-shIFITM3 or -shNCon cells were infected with pseudoviruses (1×10^5 TCID50/mL) harboring H5 for 48 h. **B–C** Quantitation of H5N9 or H7N9 pseudoviruses entry by determining luciferase activity in cell lysates. MDCK-Tet3G-IFITM3 (**B**) and HEK293-Tet3G-IFITM3 (**C**) cells (2×10^4 cell/well, 96-well plate) treated with Dox or DMSO (5 μg/mL) were inoculated with pseudotyped viruses harboring H5 or H7 (MOI = 1.0) for 48 h. The data are presented as means ± SD (n = 6). **D** Co-localization of IFITM3 and hemagglutinin (HA). The plasmids expressing IFITM3-mCherry and H5-EGFP or H7-EGFP were co-transfected (2 μg/well each plasmid, 6-well plate) into HEK293T cells for 48 h, and the cells were fixed for imaging analysis by laser confocal microscope (63×, oil). **E** Western blotting analysis of the expression of C-terminally EGFP-tagged HA (H5-EGFP and H7-EGFP) using an anti-EGFP antibody, and β-actin acts as the loading control. **F-G** Interaction analysis of IFITM3 with H5 (**C**) or H7 (**D**) by anti-mCherry co-immunoprecipitation (Co-IP). The HEK293T cells were transfected with the indicated plasmids for 48 h before Co-IP, and mCherry was used as a negative control. The lysates and immunoprecipitates were detected by Western blotting with the indicated antibodies. The experiments were repeated twice and yielded similar results. *, $P < 0.05$; **, $P < 0.01$; ***, $P < 0.001$.

pmCherry-N1 to encode various fragments with the C-terminally mCherry tag (Fig. 4A). The intracellular localization analysis of HA_2 fragments in HeLa cells showed that ΔFP_HA_2 fragments lacked FP but included the TM domain that was resided in late endosomal and lysosomal organelles by eco-labeling with markers Rab7 and LAMP1 (Fig. 4B, upper panels), and this was similar to the wild-type HA_2 subunit. However, the absence of the TM domain resulted in the disappearance of this localization (Fig. 4B, lower panels). Moreover, the fluorescent IFITM3 had almost complete co-localization with ΔFP_H5_2 or ΔFP_H7_2 fragment that lacked the fusion peptide but included TM domain but less co-location with ΔTM_H5_2 or ΔTM_H7_2 fragment lacking TM domain but including FP (Fig. 4C), providing a space basis for IFITM3 to kidnap the TM domain of HA. In immunoprecipitation analysis, IFITM3-EGFP demonstrated a strong binding affinity to the ΔFP_H5_2 or ΔFP_H7_2 fragment lacking fusion peptide, but including the stalk domain transmembrane domain, and conversely, EGFP has no binding activity (Fig. 4D). In addition, IFITM3-EGFP showed a faint binding to ΔTM_H5_2 or ΔTM_H7_2 fragment that lacked the transmembrane domain but included fusion peptide and stalk domain (Fig. 4D). However, the stalk fragment of the HA_2 subunit was not responsible for their interaction (Fig. 4E). Altogether, these results demonstrated a specific interaction between IFITM3 and the transmembrane domain of the HA_2 subunit.

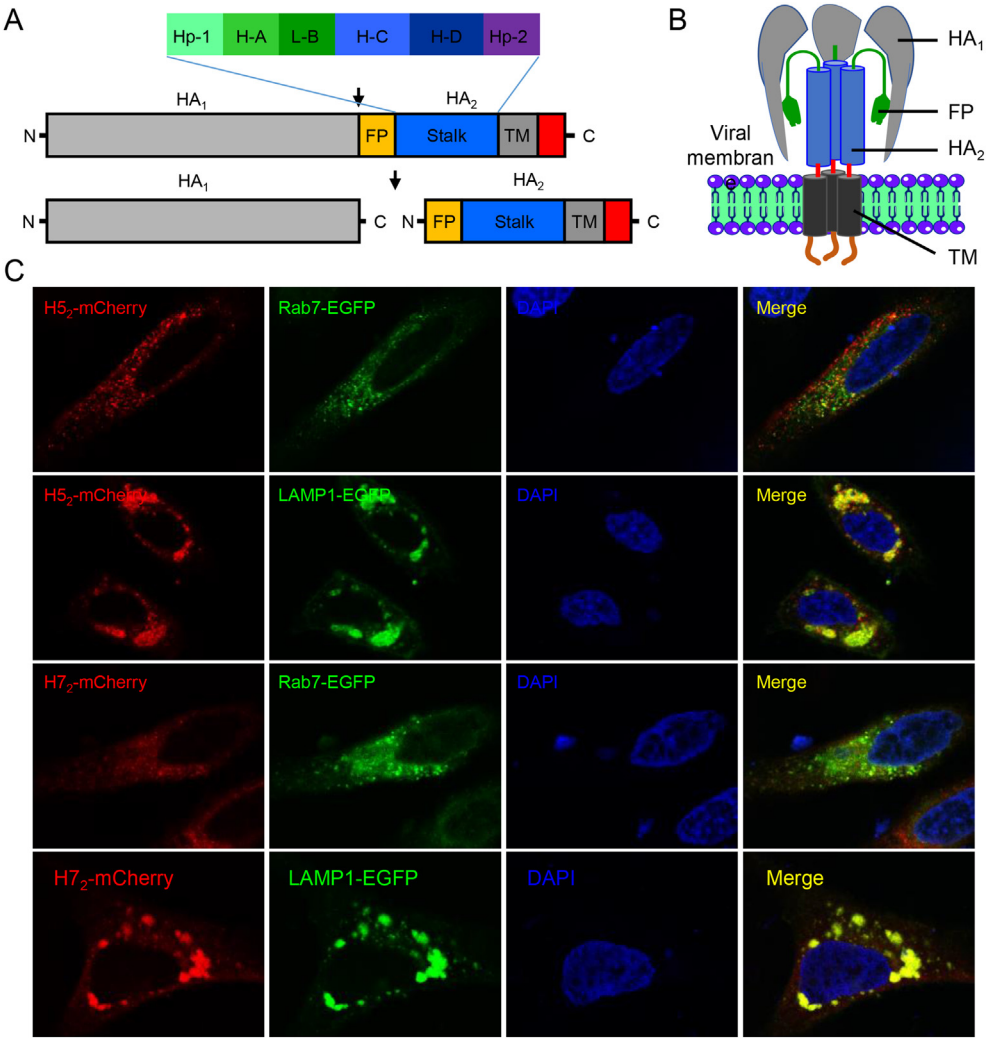

Fig. 2. Subcellular localization analysis of HA_2 subunit in late endosomes. **A** Schematic diagram of HA. HA precursor is divided into two subunits by proteolytic cleavage. HA_2 contains fusion peptide (FP), stem region (stalk), transmembrane domain (TM), and C-terminus. **B** Schematic diagram of HA on the surface of influenza virus particles. **C** Localization of $H5_2$ or $H7_2$ subunit. HeLa cells were co-transfected with the plasmids which expressing $H5_2$- or $H7_2$-mCherry and Rab7-EGFP or LAMP1-EGFP (2 μg/well each plasmid, 6-well plate), followed by imaging analysis by laser confocal microscope (63×, oil).

3.5. Transmembrane domain of IFITM3 is responsible for its interaction with the HA2 subunit

The feature of IFITM3 topology contains five domains: a cytosolic N terminus (NTD), an intramembrane domain (IMD), a cytosolic conserved intracellular loop (CIL) domain, a transmembrane domain (TMD) and extracellular C terminus (CTD) (Fig. 5A) (Yánez et al., 2020). The IMD and CIL domains are highly conserved to form the CD225 domain (John et al., 2013). Each domain and the correct subcellular localization of IFITM3 are key factors of its antiviral activity (Rahman et al., 2020). So, it is still a question about which domain is involved in its interaction with the HA_2 subunit. To answer this question, a series of EGFP-tagged IFITM3-truncated mutants were constructed to encode various fragments with C-terminally EGFP (Fig. 5A). Also, the EGFP-fused NTD and CIL-TMD fragments were highly expressed, while IMD-CIL-EGFP expression was slightly lower (Fig. 5B). After that, mCherry-tagged HA_2 subunit with NTD, IMD-CIL, and CIL-TMD fragments was expressed in HEK293T cells, and the expression of the interest proteins was detected with anti-mCherry or EGFP antibodies by Western blotting (Fig. 5C and D). Immunoprecipitation analyses demonstrated that mCherry-tagged $H5_2$ and $H7_2$ have efficiently co-precipitated with CIL-TMD fragment of IFITM3 but did not interact with the NTD domain (Fig. 5D). Surprisingly, a weaker interaction between IMD-CIL in IFITM3 with $H5_2$ was observed, but not with the $H7_2$ subunit (Fig. 5D). Localization analyses showed that the $H5_2$ subunit showed co-localization with the IFITM3 CIL-TMD fragment but not the IMD-CIL fragment, while the $H7_2$ subunit had partial co-localization (Fig. 5E). These results seemed to imply that the transmembrane structure of IFITM3 plays an important role in its interaction with HA.

Next, ΔFP_$H5_2$, ΔTM_$H5_2$, ΔFP_$H7_2$, or ΔTM_$H7_2$ was co-precipitated with IMD-CIL or CIL-TMD fragment of IFITM3. Co-immunoprecipitation experiments showed that the FP-deficient $H5_2$ subunit was co-precipitated with IMD-CIL (CD225 domain) and CIL-TMD domain (Fig. 5F). Similarly, the TM-deficient $H5_2$ subunit was also captured by IMD-CIL (CD225 domain) or CIL-TMD domain, respectively, but the affinity between them remained weak (Fig. 5F) and consistent with that shown in Fig. 5D. Localization analyses showed that TM-deficient or FP-deficient $H5_2$ subunit showed partial co-localization with the IFITM3 IMD-CIL fragment and FP-deficient $H5_2$ subunit co-localization with IFITM3 CIL-TMD fragment, while TM deletion mutation resulted in the disappearance of this co-localization (Fig. 5H). Meanwhile, the FP-deficient $H7_2$ subunit was co-precipitated with the CIL-TMD domain

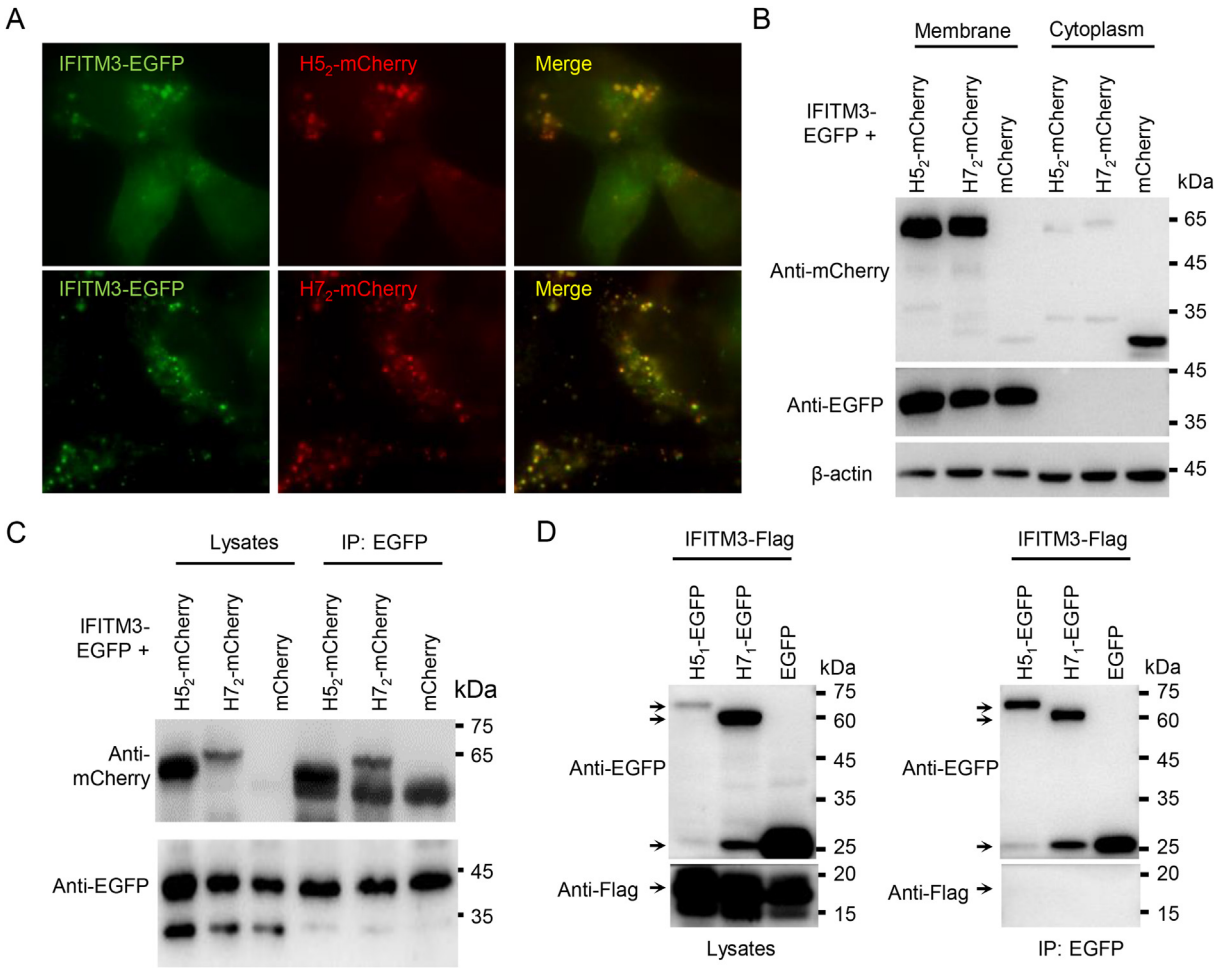

Fig. 3. Interaction between IFITM3 and HA_2 subunit. **A** Co-localization of IFITM3 and $H5_2$ or $H7_2$ subunit in HEK293T as described in Fig. 1D. **B** Isolation and identification of the membrane proteins containing IFITM3 and $H5_2$ or $H7_2$ by Western blotting. β-actin was used as a loading control. **C** Validation of IFITM3 interaction with $H5_2$ or $H7_2$ subunit in the isolated membrane proteins as in (**B**) by anti-EGFP magnetic beads. **D** IFTM3 protein cannot be captured by the HA_1 subunit of H5 or H7. HEK293T cells (1×10^6 cell/well, 6-well plate) were co-transfected with the plasmids expressing $H5_1$-EGFP or $H7_1$-EGFP and IFITM3-Flag (2 μg/well each plasmid) respectively for 48 h before Co-IP with anti-EGFP magnetic beads, the plasmid vector pEGFP-N3 was used as negative control.

but not with the IMD-CIL domain, and TM deletion mutant (ΔTM_$H7_2$) did not bind with the CIL-TMD domain in IFITM3 (Fig. 5G). In terms of subcellular localization, TM-deficient or FP-deficient $H7_2$ subunit partly co-localized with IFITM3 IMD-CIL or CIL-TMD domain (Fig. 5H), providing favorable conditions for the interaction between them. To sum up, the transmembrane domain of IFITM3 was required for IFITM3-HA_2 subunit interaction. According to the above data, the transmembrane domain of IFITM3 and HA protein is supported to mediate their interaction.

3.6. IFITM3 interacts with HA_2 subunit from other subtypes of influenza A virus and influenza B virus

To further verify this interaction, the recombinant expression plasmids encoding EGFP-fused HA_2 from other subtypes of influenza A virus and influenza B virus, including H1, H2, H3, H9, H10, and HB, were constructed to express the corresponding target protein. The immunoprecipitation analysis of IFITM3-mCherry and this HA_2-EGFP was performed with anti-mCherry agarose beads. The results showed that IFITM3 could capture this HA_2 subunit of other HA subtypes such as H1, H2, H3, H9, and H10 and HA of influenza B virus (Fig. 6A and B). To circumvent the macromolecular tag EGFP, the recombinant plasmids of HA_2 fused C-Myc were constructed for immunoprecipitation with anti-GFP magnetic beads. As shown in Fig. 6B, IFITM3-EGFP could also capture these Myc-tagged HA_2 subunits respectively (Fig. 6C–E), indicating the interaction between IFITM3 and HA_2 subunit is not affected by the tagged protein. In addition, we found that the binding ability of HA_2 from different subtypes to IFITM3 was different. Whether this difference is related to the inhibitory ability of IFITM3 to different subtypes of influenza virus remains to be verified. Altogether, the above results supported that IFITM3 interacts with the HA_2 subunit of HA, which might be a novel mechanism of IFITM3 restriction to viral membrane fusion (Fig. 6F).

4. Discussion

IFITMs have been confirmed to play an important role in a variety of physiological or pathological processes. For example, IFITM2 and IFITM3 can participate in the differentiation of Th1/Th2 T cells (Yánez et al., 2020), and the host antiviral immune response (Ren et al., 2020), while IFITM5 regulates the development and maturation of bone cells and germ cells (Tanaka et al., 2005; Hanagata et al., 2011). However, little is known about the molecular mechanism of their antiviral activity. For IFITM3, previous studies have shown that it shows different degrees of resistance to different viruses, and even has no inhibitory effect or promotes infection, such as murine leukemia virus (MuLV), Lassa virus (LASV) and Junin virus (JUNV), lymphocytic choroid plexus meningitis virus (LCMV), and Crimean-Congo hemorrhagic fever (CCHFV) and some

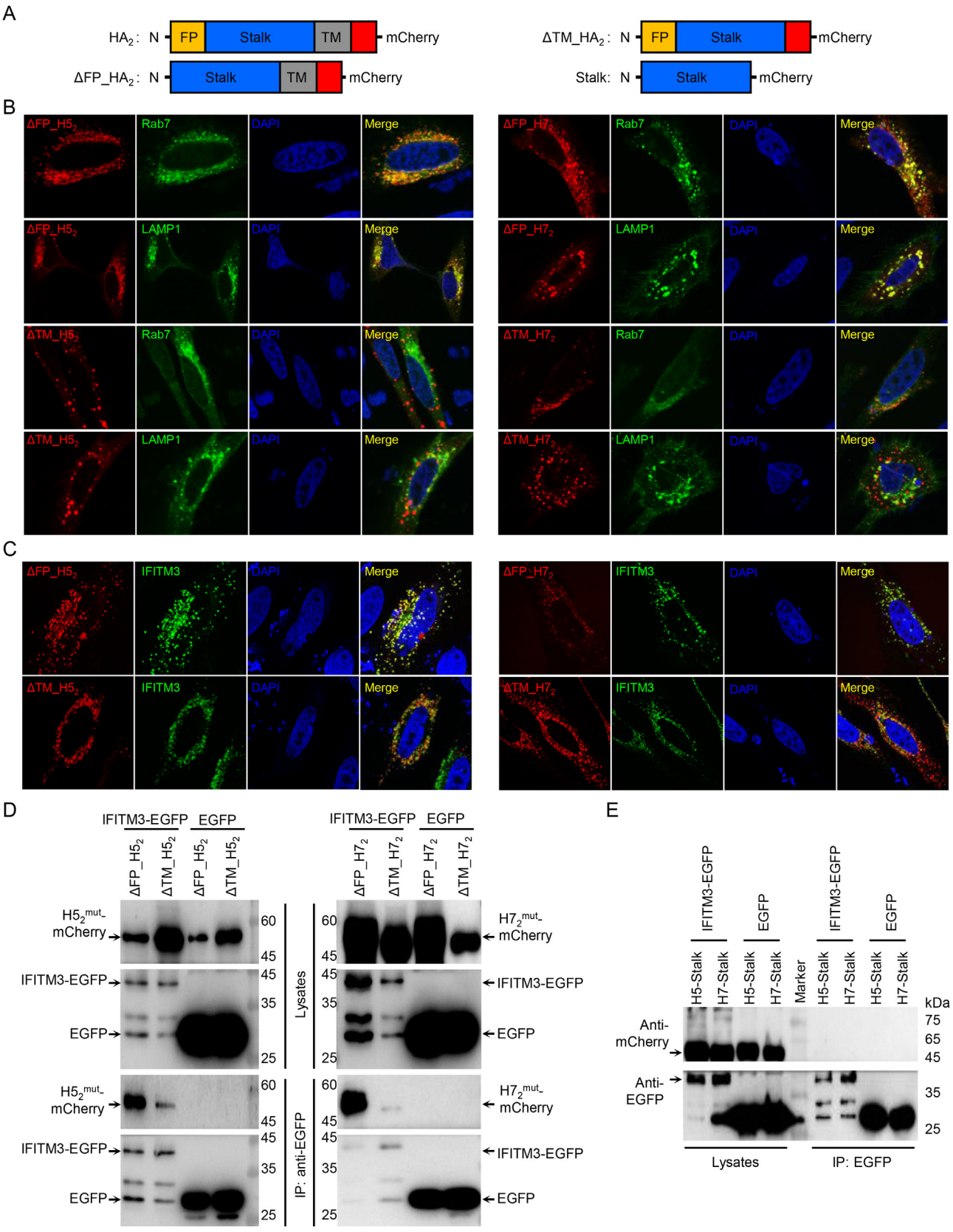

Fig. 4. IFITM3 interacts with the HA_2 subunit based on the transmembrane domain of HA. **A** The truncated variants of the HA_2 subunit are depicted. **B** Localization of truncated variants of $H5_2$ or $H7_2$ subunit. HeLa cells co-transfected with the plasmids which expressing ΔFP_$H5_2$-, ΔFP_$H7_2$-, ΔTM_$H5_2$- or ΔTM_$H7_2$-mCherry and Rab7-EGFP or LAMP1-EGFP respectively (2 μg/well each plasmid, 6-well plate), followed by imaging analysis by laser confocal microscope (63×, oil). **C** Co-localization of IFITM3 and the truncated variants of $H5_2$ or $H7_2$ subunit. **D** The interaction of IFITM3 with the truncated variants of $H5_2$ or $H7_2$ subunit by Co-IP anti-EGFP magnetic beads. **E** IFTM3 protein was identified for not capturing the stalk region of $H5_2$ or $H7_2$ subunit in HEK293T cells co-transfected with IFITM3-fusion expression plasmid and the stalk truncate of $H5_2$ or $H7_2$ respectively for 48 h by Co-IP with anti-EGFP magnetic beads.

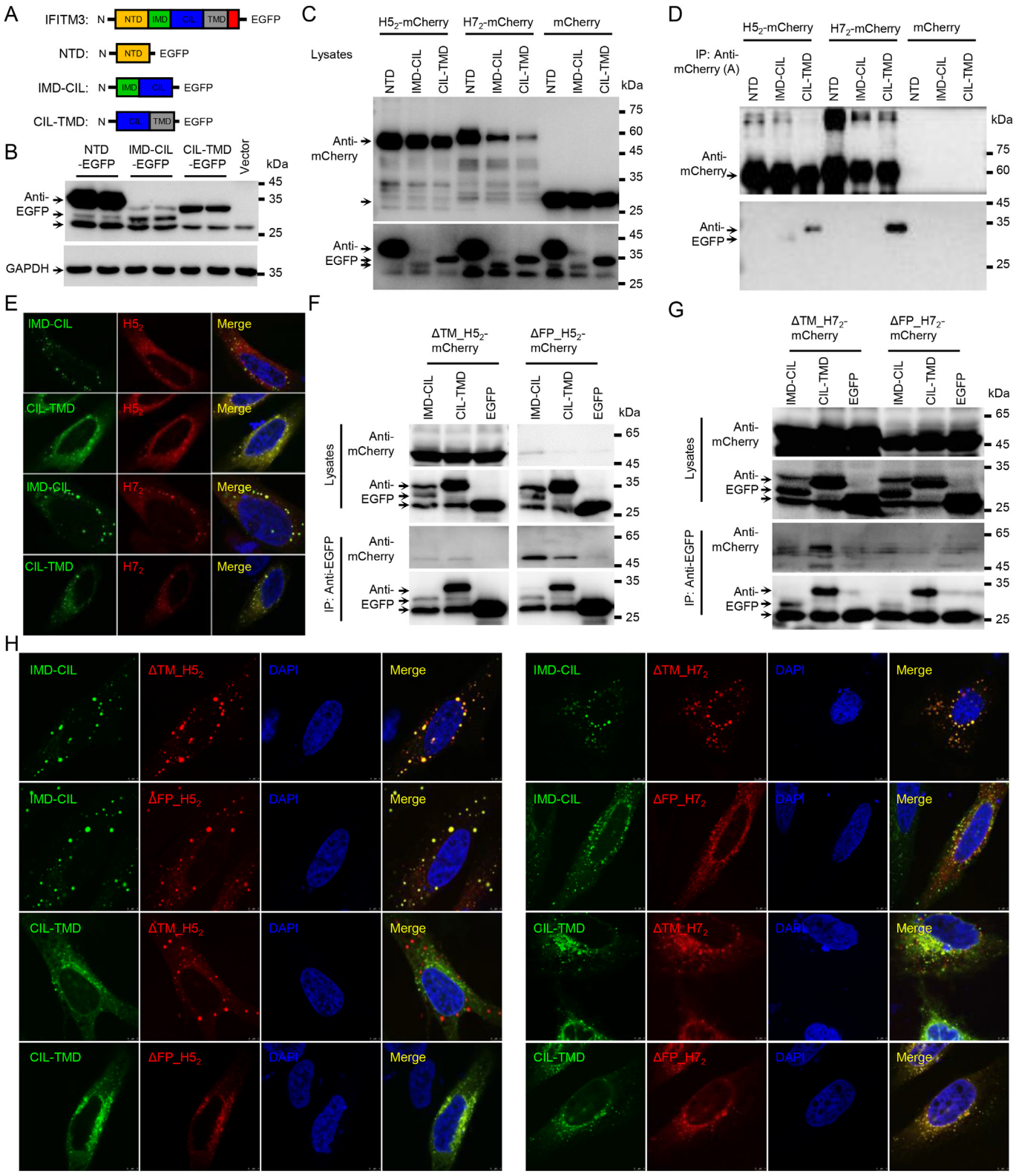

Fig. 5. Interaction of IFITM3 with HA_2 subunit mediated by its transmembrane domain. **A** The truncated variants of IFITM3 protein are depicted. **B** The expression of IFITM3-truncated mutants was detected by Western blotting. **C–D** The interaction of IFITM3-truncated variants with $H5_2$ or $H7_2$ subunit. HEK293T cells (1×10^6 cell/well, 6-well plate) were co-transfected with $H5_2$ or $H7_2$-fusion expression plasmids and each IFITM3 truncate respectively (2 μg/well each plasmid, 6-well plate) for 48 h before Co-IP with anti-mCherry beads. The lysates (**C**) and immunoprecipitates (**D**) were measured with the indicated antibodies by Western blotting. **E** Co-localization of IFITM3-truncated mutants (IMD-CIL and CIL-TMD) and $H5_2$ or $H7_2$ subunit in HeLa cells. (**F–G**) The interaction of IFITM3-truncated mutants with the truncated variants of the $H5_2$ (**F**) or $H7_2$ (**G**) subunit was verified by Co-IP with anti-EGFP magnetic beads. **H** Co-localization of IFITM3-truncated mutants and the truncated $H5_2$ or $H7_2$ subunit variants in HeLa cells.

DNA viruses (Brass et al., 2009; Warren et al., 2014). Furthermore, endogenous IFITM3 can also promote some viral infections such as coronavirus OC43 (Zhao et al., 2014), cytomegalovirus (HCMV) (Xie et al., 2015) and severe acute respiratory syndrome coronavirus 2 (SARS-CoV-2) (Prelli Bozzo et al., 2021) infection. Equally important, its antiviral activity varies among different types of cells (Narayana et al., 2015). However, it is unclear what factors mediate the functional differences of IFITM3 during virus infection or host defense. In the past, IFITM3 was thought to work through a universal mechanism due to its broad antiviral spectrum, including changing the physicochemical characteristics of the endosomal lumen (Goraya et al., 2020), increasing the inflexibility of the cellular or endosomal membrane (Chemudupati et al., 2019), or interacting with host cellular factors such as itself (Winkler et al., 2019) or VAPA (Amini-Bavil-Olyaee et al., 2013). Therefore, IFITM3 could play the role of antiviral function through various mechanisms.

Increasing evidence has suggested that IFITM3 inhibits virus entry and infection by blocking the membrane fusion of many enveloped viruses. Recent studies have suggested that IFITM3 interacts with Env (gp160 or gp120 protein) of human immunodeficiency virus-1 (HIV-1) strains that IFITM3 inhibits and, in contrast, cannot bind to the Env of HIV-1 strains that are not inhibited by IFITM3 (Drouin et al., 2020), and this interaction might occur in the Golgi apparatus. Unlike the HIV-1 virus, the influenza virus enters the endosomes through endocytosis, which triggers the conformational changes of HA protein at low pH in late endosomes to initiate membrane fusion (Boonstra et al., 2018). In addition, IFITMs overexpression could blocks SARS-CoV-2 infection, but SARS-CoV-2 spike protein has been confirmed to hijack endogenous IFITMs by binding their N-terminal region to promote virus for efficient infection (Buchrieser et al., 2021; Peacock et al., 2021; Prelli Bozzo et al., 2021; Rajah et al., 2021; Shi et al., 2021). In our study, the interaction between IFITM3 and influenza virus HA protein was further investigated. We found that IFITM3 inhibited the HA-mediated viral entry and partial co-localized with HA protein in late endosomes and lysosomes, which might be a novel mechanism of IFITM3 restriction on viral membrane fusion. Future studies should focus on whether this mechanism is a common antiviral mechanism of IFITM3 against enveloped viruses, which might provide theoretical support for its applied research.

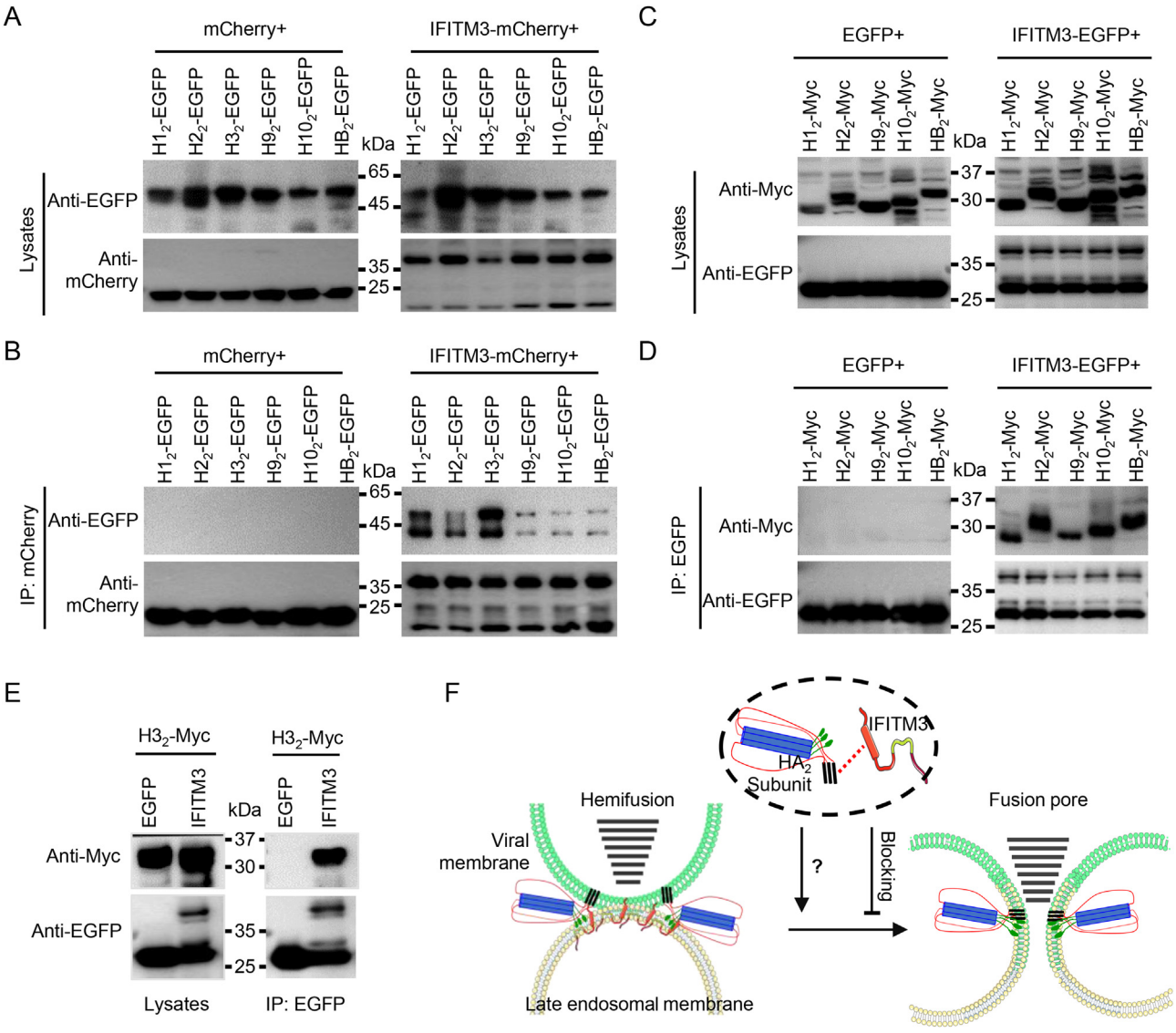

Fig. 6. IFITM3 binds the HA_2 subunit directly from other subtypes of influenza A and B viruses. **A–B** Interaction analysis of IFITM3 with C-terminally EGFP-tagged HA_2 subunit of H1, H2, H3, H9, H10, and HB by anti-mCherry Co-IP. The HEK293T cells lysates (**A**) and immunoprecipitates (**B**) were detected by Western blotting with the indicated antibodies. **C–E** Validation of IFITM3 binding C-terminally Myc-tagged HA_2 subunit of H1, H2, H3, H9, H10, and HB by anti-EGFP magnetic beads. **F** Schematic diagram of the interaction of HA_2 subunits with IFITM3. The interaction between IFITM3 and HA_2 subunit may occur during virus-late endosomal membrane fusion, but its specific biological significance needs to be further explored.

Previous study showed that IFITM3 limited the formation and expansion of the fusion pore of the influenza virus-endosomal membrane through proximity mechanism rather than inhibiting the lipid-mixing stage (hemifusion) of viral fusion (Desai et al., 2014). Indeed, *in vitro* expression showed that IFITM3 demonstrated partial co-localization with HA in this study. HA protein was cleaved into two distinct subunits (HA_1 and HA_2) during viral entry. HA_1 subunit is considered responsible for binding to the host cell membrane to initiate endocytosis, while HA_2 controls the fusion between the viral membrane and endosomal membrane (Kim et al., 2011; Hamilton et al., 2012). At the beginning of membrane fusion, the C-terminal transmembrane domain of HA_2 was anchored to the viral membrane. The fusion peptide signal on N-terminal regions of HA_2 exposes and inserted into the host cell membrane (Kim et al., 2011; Hamilton et al., 2012). There are several intermediate steps during the fusion process, and the fusion peptide and transmembrane domain are co-localized in the same membrane. Also, FP and the transmembrane domain interact to facilitate pore formation. Therefore, we hypothesized that IFITM3 might interact with the HA_2 subunit. Importantly, this hypothesis was confirmed at the cellular level using the truncations containing the respective major domains of IFITM3 or HA protein, and this interaction between IFITM3 and HA_2 subuint is mediated by their transmembrane domain. However, the biological significance of the interaction between IFITM3 and viral envelope proteins needs to be further explored in host antiviral defense or viral antagonism or escape, for example, the interaction of N-terminal region of IFITM with SARS-CoV-2 S protein has been proved to promote SARS-CoV-2 fusion predominantly in early endosomes (Prelli Bozzo et al., 2021).

Although the topology structure has not been fully resolved, IFITM3 is characterized as a single-pass type II membrane protein (Bailey C.C. et al., 2013) and is divided into five main domains: a variable and hydrophobic N-terminal domain (NTD), a conservative and hydrophobic intramembrane domain (IMD), a conserved intracellular loop (CIL), a hydrophobic transmembrane domain (TMD), and a short and highly variable C-terminal domain (CTD) (Weston et al., 2014). NTD and CIL are distributed in the cytoplasm, and CTD is located in the endosomal lumen (Sun F. et al., 2020). The internalization and translocation of IFITM3 to endosomes are mediated through the YEML motif present in the N-terminal (Jia et al., 2014). Palmitoylation on the membrane-proximal cysteines of IFITM3 protein is confirmed to control its clustering in membrane compartments and antiviral activity against the influenza virus (Yount et al., 2010, 2012). IFITM3 phosphorylation at Y20 prevents endocytosis and degradation, resulting in loss of antiviral activity (Chesarino N. M. et al., 2014). More than that, the polymorphisms associated with IFITM3, such as rs12252 and rs34481144 encoding different truncated genetic variants, showed association with increased severity in SARS-CoV-2 (Zhang et al., 2020; Li et al., 2022), IAV (Allen et al., 2017), hantaan virus (HTNV) (Xu-Yang et al., 2016), chikungunya virus (CHIKV) (Franz et al., 2021), and HIV-1 (Zhang Y. et al., 2015) and so on. Therefore, these findings suggest that appropriate subcellular localization and protein integrity are considered essential for the antiviral activity of IFITM3. The truncated analyses in our study revealed that the transmembrane domain of IFITM3 was responsible for its interaction with influenza virus HA protein. However, the affinity of IFITM3 to the HA_2 subunit of different serotypes of influenza virus such as H5 or H7 is also different in our study. Previous study and our data showed the different inhibition activities of IFITM3 on HA-mediated virus infection of different serotypes (Huang I. C. et al., 2011). Taken together, these data suggest that the difference in affinity of IFITM3 to different HA_2 subunits may be related to the susceptibility of different serotypes of influenza virus to IFITM3 inhibition, which needs to be further verified.

5. Conclusions

In summary, the interaction of IFITM3 with the HA_2 subunit from H5 and H7 subtypes was reported for the first time. It was showed that the restriction of IFITM3 on the viral membrane fusion might rely on the transmembrane domain. Moreover, the interaction of IFITM3 has been verified with the HA_2 subunit of other HA subtypes such as H1, H2, H3, H9, and H10, and HA of influenza B virus. Therefore, a new possible antiviral mechanism or mode of IFITM3 was proposed through our research that restricts membrane fusion by interacting with the viral fusion protein. Future studies should focus on whether this mechanism is a common antiviral mechanism of IFITM3 against enveloped viruses to provide more theoretical support for its applied research.

Data availability

All data relevant to the study are included in the article or uploaded as supplementary information. Additional data are available from the corresponding author on reasonable request.

Ethics statement

This article does not contain any studies with human or animal subjects performed by any of the authors.

Author contributions

Wang Xu: methodology, validation, data curation, and original draft writing. Yuhang Wang: methodology, formal analysis. Letian Li: validation, formal analysis. Xiaoyun Qu: validation. Quan Liu: validation. Tiyuan Li: validation. Shipin Wu: validation. Ningyi Jin: conceptualization and funding acquisition. Ming Liao: formal analysis and data curation. Shouwen Du: conceptualization, methodology, validation, and writing the original draft. Chang Li: conceptualization, formal analysis, writing-reviewing or editing, funding acquisition, and supervision.

Conflict of interest

The authors declare that they have no conflict of interest.

Acknowledgments

This work was supported by the National Natural Science Foundation of China (31702210, 31972719) and the CAMS Innovation Fund for Medical Sciences (2020–12M-5-001).

References

Allen, E., Randolph, A., Bhangale, T., Dogra, P., Ohlson, M., Oshansky, C., Zamora, A., Shannon, J., Finkelstein, D., Dressen, A., Devincenzo, J., Caniza, M., Youngblood, B., Rosenberger, C., Thomas, P., 2017. SNP-mediated disruption of CTCF binding at the IFITM3 promoter is associated with risk of severe influenza in humans. Nat. Med. 23, 975–983.

Amini-Bavil-Olyaee, S., Choi, Y., Lee, J., Shi, M., Huang, I., Farzan, M., Jung, J., 2013. The antiviral effector IFITM3 disrupts intracellular cholesterol homeostasis to block viral entry. Cell Host Microbe 13, 452–464.

Bailey, C., Kondur, H., Huang, I., Farzan, M., 2013. Interferon-induced transmembrane protein 3 is a type II transmembrane protein. J. Biol. Chem. 288, 32184–32193.

Bailey, C.C., Huang, I.C., Kam, C., Farzan, M., 2012. Ifitm3 limits the severity of acute influenza in mice. PLoS Pathog. 8, e1002909.

Boonstra, S., Blijleven, J., Roos, W., Onck, P., Van Der Giessen, E., Van Oijen, A., 2018. Hemagglutinin-mediated membrane fusion: a biophysical perspective. Annu. Rev. Biophys. 47, 153–173.

Brass, A.L., Huang, I.C., Benita, Y., John, S.P., Krishnan, M.N., Feeley, E.M., Ryan, B.J., Weyer, J.L., Van Der Weyden, L., Fikrig, E., Adams, D.J., Xavier, R.J., Farzan, M., Elledge, S.J., 2009. The IFITM proteins mediate cellular resistance to influenza A H1N1 virus, West Nile virus, and dengue virus. Cell 139, 1243–1254.

Buchrieser, J., Dufloo, J., Hubert, M., Monel, B., Planas, D., Rajah, M.M., Planchais, C., Porrot, F., Guivel-Benhassine, F., Van Der Werf, S., Casartelli, N., Mouquet, H., Bruel, T., Schwartz, O., 2021. Syncytia formation by SARS-CoV-2-infected cells. EMBO J. 40, e107405.

Cao, T.T., Du, S.W., Xu, W., Xing, B., Zhao, F., Wang, M.P., Zhu, Y.L., Bai, J.Y., Tian, Y.F., Liu, L.M., Zhao, C.Q., Zhou, Y.F., Li, C., Jin, N.Y., 2017. Establishment and functional analysis of MDCK cell line induced IFITM3 expression based on tet-on 3G system. Chem. J. Chin. Univ. 38, 770–777.

Chang, D., Cheng, S., Kantchev, E., Lin, C., Liu, Y., 2008. Membrane interaction and structure of the transmembrane domain of influenza hemagglutinin and its fusion peptide complex. BMC Biol. 6, 2.

Chemudupati, M., Kenney, A.D., Bonifati, S., Zani, A., Mcmichael, T.M., Wu, L., Yount, J.S., 2019. From APOBEC to ZAP: diverse mechanisms used by cellular restriction factors to inhibit virus infections. Biochimica et biophysica acta. Mol. Cell Res. 1866, 382–394.
Chesarino, N.M., Compton, A.A., Mcmichael, T.M., Kenney, A.D., Zhang, L., Soewarna, V., Davis, M., Schwartz, O., Yount, J.S., 2017. IFITM3 requires an amphipathic helix for antiviral activity. EMBO Rep. 18, 1740–1751.
Chesarino, N.M., Mcmichael, T.M., Hach, J.C., Yount, J.S., 2014. Phosphorylation of the antiviral protein interferon-inducible transmembrane protein 3 (IFITM3) dually regulates its endocytosis and ubiquitination. J. Biol. Chem. 289, 11986–11992.
Compton, A.A., Bruel, T., Porrot, F., Mallet, A., Sachse, M., Euvrard, M., Liang, C., Casartelli, N., Schwartz, O., 2014. IFITM proteins incorporated into HIV-1 virions impair viral fusion and spread. Cell Host Microbe 16, 736–747.
Coomer, C., Rahman, K., Compton, A., 2021. CD225 proteins: a family portrait of fusion regulators. Trends Genet. 37, 406–410.
Desai, T.M., Marin, M., Chin, C.R., Savidis, G., Brass, A.L., Melikyan, G.B., 2014. IFITM3 restricts influenza A virus entry by blocking the formation of fusion pores following virus-endosome hemifusion. PLoS Pathog. 10, e1004048.
Drouin, A., Migraine, J., Durand, M., Moreau, A., Burlaud-Gaillard, J., Beretta, M., Roingeard, P., Bouvin-Pley, M., Braibant, M., 2020. Escape of HIV-1 envelope glycoprotein from the restriction of infection by IFITM3. J. Virol. 95 e01994-20.
Everitt, A.R., Clare, S., Pertel, T., John, S.P., Wash, R.S., Smith, S.E., Chin, C.R., Feeley, E.M., Sims, J.S., Adams, D.J., Wise, H.M., Kane, L., Goulding, D., Digard, P., Anttila, V., Baillie, J.K., Walsh, T.S., Hume, D.A., Palotie, A., Xue, Y., Colonna, V., Tyler-Smith, C., Dunning, J., Gordon, S.B., Gen, I.I., Investigators, M., Smyth, R.L., Openshaw, P.J., Dougan, G., Brass, A.L., Kellam, P., 2012. IFITM3 restricts the morbidity and mortality associated with influenza. Nature 484, 519–523.
Floyd, D.L., Ragains, J.R., Skehel, J.J., Harrison, S.C., Van Oijen, A.M., 2008. Single-particle kinetics of influenza virus membrane fusion. Proc. Natl. Acad. Sci. U. S. A. 105, 15382–15387.
Foster, T., Wilson, H., Iyer, S., Coss, K., Doores, K., Smith, S., Kellam, P., Finzi, A., Borrow, P., Hahn, B., Neil, S., 2016. Resistance of transmitted founder HIV-1 to IFITM-mediated restriction. Cell Host Microbe 20, 429–442.
Franz, S., Pott, F., Zillinger, T., Schuler, C., Dapa, S., Fischer, C., Passos, V., Stenzel, S., Chen, F., Dohner, K., Hartmann, G., Sodeik, B., Pessler, F., Simmons, G., Drexler, J.F., Goffinet, C., 2021. Human IFITM3 restricts chikungunya virus and Mayaro virus infection and is susceptible to virus-mediated counteraction. Life Sci Alliance 4, e202000909.
Goraya, M.U., Zaighum, F., Sajjad, N., Anjum, F.R., Sakhawat, I., Rahman, S.U., 2020. Web of interferon stimulated antiviral factors to control the influenza A viruses replication. Microb. Pathog. 139, 103919.
Guo, X., Steinkuhler, J., Marin, M., Li, X., Lu, W., Dimova, R., Melikyan, G.B., 2021. Interferon-induced transmembrane protein 3 blocks fusion of diverse enveloped viruses by altering mechanical properties of cell membranes. ACS Nano 15, 8155–8170.
Hamilton, B.S., Whittaker, G.R., Daniel, S., 2012. Influenza virus-mediated membrane fusion: determinants of hemagglutinin fusogenic activity and experimental approaches for assessing virus fusion. Viruses 4, 1144–1168.
Hanagata, N., Li, X., Morita, H., Takemura, T., Li, J., Minowa, T., 2011. Characterization of the osteoblast-specific transmembrane protein IFITM5 and analysis of IFITM5-deficient mice. J. Bone Miner. Metabol. 29, 279–290.
Hay, A.J., Gregory, V., Douglas, A.R., Lin, Y.P., 2001. The evolution of human influenza viruses. Philos. Trans. R. Soc. Lond. B Biol. Sci. 356, 1861–1870.
Hensen, L., Matrosovich, T., Roth, K., Klenk, H.D., Matrosovich, M., 2019. HA-dependent tropism of H5N1 and H7N9 influenza viruses to human endothelial cells is determined by reduced stability of the HA, which allows the virus to cope with inefficient endosomal acidification and constitutively expressed IFITM3. J. Virol. 94 e01223-19.
Huang, D.L., Li, Y., Liang, J., Yu, L., Xue, M., Cao, X.X., Xiao, B., Tian, C.L., Liu, L., Zheng, J.S., 2020. The new salicylaldehyde S,S-propanedithioacetal ester enables N-to-C sequential native chemical ligation and ser/thr ligation for chemical protein synthesis. J. Am. Chem. Soc. 142, 8790–8799.
Huang, I.C., Bailey, C.C., Weyer, J.L., Radoshitzky, S.R., Becker, M.M., Chiang, J.J., Brass, A.L., Ahmed, A.A., Chi, X., Dong, L., Longobardi, L.E., Boltz, D., Kuhn, J.H., Elledge, S.J., Bavari, S., Denison, M.R., Choe, H., Farzan, M., 2011. Distinct patterns of IFITM-mediated restriction of filoviruses, SARS coronavirus, and influenza A virus. PLoS Pathog. 7, e1001258.
Jia, R., Xu, F., Qian, J., Yao, Y., Miao, C., Zheng, Y.M., Liu, S.L., Guo, F., Geng, Y., Qiao, W., Liang, C., 2014. Identification of an endocytic signal essential for the antiviral action of IFITM3. Cell Microbiol. 16, 1080–1093.
John, S., Chin, C., Perreira, J., Feeley, E., Aker, A., Savidis, G., Smith, S., Elia, A., Everitt, A., Vora, M., Pertel, T., Elledge, S., Kellam, P., Brass, A., 2013. The CD225 domain of IFITM3 is required for both IFITM protein association and inhibition of influenza A virus and dengue virus replication. J. Virol. 87, 7837–7852.
Kenney, A.D., Mcmichael, T.M., Imas, A., Chesarino, N.M., Zhang, L., Dorn, L.E., Wu, Q., Alfaour, O., Amari, F., Chen, M., Zani, A., Chemudupati, M., Accornero, F., Coppola, V., Rajaram, M.V.S., Yount, J.S., 2019. IFITM3 protects the heart during influenza virus infection. Proc. Natl. Acad. Sci. U. S. A. 116, 18607–18612.
Kim, C.S., Epand, R.F., Leikina, E., Epand, R.M., Chernomordik, L.V., 2011. The final conformation of the complete ectodomain of the HA2 subunit of influenza hemagglutinin can by itself drive low pH-dependent fusion. J. Biol. Chem. 286, 13226–13234.
Kummer, S., Avinoam, O., Krausslich, H.G., 2019. IFITM3 clusters on virus containing endosomes and lysosomes early in the influenza A infection of human airway epithelial cells. Viruses 11, 548.
Lai, A., Freed, J., 2015. The interaction between influenza HA fusion peptide and transmembrane domain affects membrane structure. Biophys. J. 109, 2523–2536.
Lanz, C., Schotsaert, M., Magnus, C., Karakus, U., Hunziker, A., Sempere Borau, M., Martinez-Romero, C., Spieler, E.E., Gunther, S.C., Moritz, E., Hale, B.G., Trkola, A., Garcia-Sastre, A., Stertz, S., 2021. IFITM3 incorporation sensitizes influenza A virus to antibody-mediated neutralization. J. Exp. Med. 218, e20200303.
Li, Y., Wei, L., He, L., Sun, J., Liu, N., 2022. Interferon-induced transmembrane protein 3 gene polymorphisms are associated with COVID-19 susceptibility and severity: a meta-analysis. J. Infect. 84, 825–833.
Lin, T.Y., Chin, C.R., Everitt, A.R., Clare, S., Perreira, J.M., Savidis, G., Aker, A.M., John, S.P., Sarlah, D., Carreira, E.M., Elledge, S.J., Kellam, P., Brass, A.L., 2013. Amphotericin B increases influenza A virus infection by preventing IFITM3-mediated restriction. Cell Rep. 5, 895–908.
Majdoul, S., Compton, A.A., 2022. Lessons in self-defence: inhibition of virus entry by intrinsic immunity. Nat. Rev. Immunol. 22, 339–352.
Marziali, F., Cimarelli, A., 2021. Membrane interference against HIV-1 by intrinsic antiviral factors: the case of IFITMs. Cells 10, 1171.
Mcmichael, T.M., Zhang, L., Chemudupati, M., Hach, J.C., Kenney, A.D., Hang, H.C., Yount, J.S., 2017. The palmitoyltransferase ZDHHC20 enhances interferon-induced transmembrane protein 3 (IFITM3) palmitoylation and antiviral activity. J. Biol. Chem. 292, 21517–21526.
Narayana, S., Helbig, K., Mccartney, E., Eyre, N., Bull, R., Eltahla, A., Lloyd, A., Beard, M., 2015. The interferon-induced transmembrane proteins, IFITM1, IFITM2, and IFITM3 inhibit hepatitis C virus entry. J. Biol. Chem. 290, 25946–25959.
Nayak, D.P., Hui, E.K., Barman, S., 2004. Assembly and budding of influenza virus. Virus Res. 106, 147–165.
Peacock, T.P., Goldhill, D.H., Zhou, J., Baillon, L., Frise, R., Swann, O.C., Kugathasan, R., Penn, R., Brown, J.C., Sanchez-David, R.Y., Braga, L., Williamson, M.K., Hassard, J.A., Staller, E., Hanley, B., Osborn, M., Giacca, M., Davidson, A.D., Matthews, D.A., Barclay, W.S., 2021. The furin cleavage site in the SARS-CoV-2 spike protein is required for transmission in ferrets. Nat Microbiol 6, 899–909.
Prelli Bozzo, C., Nchioua, R., Volcic, M., Koepke, L., Kruger, J., Schutz, D., Heller, S., Sturzel, C.M., Kmiec, D., Conzelmann, C., Muller, J., Zech, F., Braun, E., Gross, R., Wettstein, L., Weil, T., Weiss, J., Diofano, F., Rodriguez Alfonso, A.A., Wiese, S., Sauter, D., Munch, J., Goffinet, C., Catanese, A., Schon, M., Boeckers, T.M., Stenger, S., Sato, K., Just, S., Kleger, A., Sparrer, K.M.J., Kirchhoff, F., 2021. IFITM proteins promote SARS-CoV-2 infection and are targets for virus inhibition in vitro. Nat. Commun. 12, 4584.
Rahman, K., Coomer, C.A., Majdoul, S., Ding, S.Y., Padilla-Parra, S., Compton, A.A., 2020. Homology-guided identification of a conserved motif linking the antiviral functions of IFITM3 to its oligomeric state. Elife 9.
Rajah, M.M., Hubert, M., Bishop, E., Saunders, N., Robinot, R., Grzelak, L., Planas, D., Dufloo, J., Gellenoncourt, S., Bongers, A., Zivaljic, M., Planchais, C., Guivel-Benhassine, F., Porrot, F., Mouquet, H., Chakrabarti, L.A., Buchrieser, J., Schwartz, O., 2021. SARS-CoV-2 Alpha, Beta, and Delta variants display enhanced Spike-mediated syncytia formation. EMBO J. 40, e108944.
Ren, L., Du, S., Xu, W., Li, T., Wu, S., Jin, N., Li, C., 2020. Current progress on host antiviral factor IFITMs. Front. Immunol. 11, 543444.
Russell, C.J., Hu, M., Okda, F.A., 2018. Influenza hemagglutinin protein stability, activation, and pandemic risk. Trends Microbiol. 26, 841–853.
Shi, G., Kenney, A., Kudryashova, E., Zani, A., Zhang, L., Lai, K., Hall-Stoodley, L., Robinson, R., Kudryashov, D., Compton, A., Yount, J., 2021. Opposing activities of IFITM proteins in SARS-CoV-2 infection. EMBO J. 40, e106501.
Skehel, J.J., Wiley, D.C., 2000. Receptor binding and membrane fusion in virus entry: the influenza hemagglutinin. Annu. Rev. Biochem. 69, 531–569.
Spence, J.S., He, R., Hoffmann, H.H., Das, T., Thinon, E., Rice, C.M., Peng, T., Chandran, K., Hang, H.C., 2019. IFITM3 directly engages and shuttles incoming virus particles to lysosomes. Nat. Chem. Biol. 15, 259–268.
Suddala, K.C., Lee, C.C., Meraner, P., Marin, M., Markosyan, R.M., Desai, T.M., Cohen, F.S., Brass, A.L., Melikyan, G.B., 2019. Interferon-induced transmembrane protein 3 blocks fusion of sensitive but not resistant viruses by partitioning into virus-carrying endosomes. PLoS Pathog. 15, e1007532.
Sun, F., Xia, Z., Han, Y., Gao, M., Wang, L., Wu, Y., Sabatier, J., Miao, L., Cao, Z., 2020a. Topology, antiviral functional residues and mechanism of IFITM1. Viruses 12, 295.
Sun, Q., Lei, N., Lu, J., Gao, R.B., Li, Z., Liu, L.Q., Sun, Y., Guo, J.F., Wang, D.Y., Shu, Y.L., 2020b. Interferon-induced transmembrane protein 3 prevents acute influenza pathogenesis in mice. Biomed. Environ. Sci. 33, 295–305.
Tanaka, S.S., Yamaguchi, Y.L., Tsoi, B., Lickert, H., Tam, P.P., 2005. IFITM/Mil/fragilis family proteins IFITM1 and IFITM3 play distinct roles in mouse primordial germ cell homing and repulsion. Dev. Cell 9, 745–756.
Tong, S., Zhu, X., Li, Y., Shi, M., Zhang, J., Bourgeois, M., Yang, H., Chen, X., Recuenco, S., Gomez, J., Chen, L.M., Johnson, A., Tao, Y., Dreyfus, C., Yu, W., Mcbride, R., Carney, P.J., Gilbert, A.T., Chang, J., Guo, Z., Davis, C.T., Paulson, J.C., Stevens, J., Rupprecht, C.E., Holmes, E.C., Wilson, I.A., Donis, R.O., 2013. New world bats harbor diverse influenza A viruses. PLoS Pathog. 9, e1003657.
Wagner, R., Matrosovich, M., Klenk, H.D., 2002. Functional balance between haemagglutinin and neuraminidase in influenza virus infections. Rev. Med. Virol. 12, 159–166.
Warren, C., Griffin, L., Little, A., Huang, I., Farzan, M., Pyeon, D., 2014. The antiviral restriction factors IFITM1, 2 and 3 do not inhibit infection of human papillomavirus, cytomegalovirus and adenovirus. PLoS One 9, e96579.

Wellington, D., Laurenson-Schafer, H., Abdel-Haq, A., Dong, T., 2019. IFITM3: how genetics influence influenza infection demographically. Biomed. J. 42, 19–26.
Weston, S., Czieso, S., White, I., Smith, S., Kellam, P., Marsh, M., 2014. A membrane topology model for human interferon inducible transmembrane protein 1. PLoS One 9, e104341.
Winkler, M., Wrensch, F., Bosch, P., Knoth, M., Schindler, M., Gärtner, S., Pöhlmann, S., 2019. Analysis of IFITM-IFITM interactions by a flow cytometry-based FRET assay. Int. J. Mol. Sci. 20, 3859.
Xie, M., Xuan, B., Shan, J., Pan, D., Sun, Y., Shan, Z., Zhang, J., Yu, D., Li, B., Qian, Z., 2015. Human cytomegalovirus exploits interferon-induced transmembrane proteins to facilitate morphogenesis of the virion assembly compartment. J. Virol. 89, 3049–3061.
Xu-Yang, Z., Pei-Yu, B., Chuan-Tao, Y., Wei, Y., Hong-Wei, M., Kang, T., Chun-Mei, Z., Ying-Feng, L., Xin, W., Ping-Zhong, W., Chang-Xing, H., Xue-Fan, B., Ying, Z., Zhan-Sheng, J., 2016. Interferon-induced transmembrane protein 3 inhibits hantaan virus infection, and its single nucleotide polymorphism rs12252 influences the severity of hemorrhagic fever with renal syndrome. Front. Immunol. 7, 535.
Yánez, D., Ross, S., Crompton, T., 2020. The IFITM protein family in adaptive immunity. Immunology 159, 365–372.
Yount, J., Karssemeijer, R., Hang, H., 2012. S-palmitoylation and ubiquitination differentially regulate interferon-induced transmembrane protein 3 (IFITM3)-mediated resistance to influenza virus. J. Biol. Chem. 287, 19631–19641.
Yount, J., Moltedo, B., Yang, Y., Charron, G., Moran, T., López, C., Hang, H., 2010. Palmitoylome profiling reveals S-palmitoylation-dependent antiviral activity of IFITM3. Nat. Chem. Biol. 6, 610–614.
Zhang, Y., Makvandi-Nejad, S., Qin, L., Zhao, Y., Zhang, T., Wang, L., Repapi, E., Taylor, S., Mcmichael, A., Li, N., Dong, T., Wu, H., 2015. Interferon-induced transmembrane protein-3 rs12252-C is associated with rapid progression of acute HIV-1 infection in Chinese MSM cohort. AIDS 29, 889–894.
Zhang, Y., Qin, L., Zhao, Y., Zhang, P., Xu, B., Li, K., Liang, L., Zhang, C., Dai, Y., Feng, Y., Sun, J., Hu, Z., Xiang, H., Knight, J., Dong, T., Jin, R., 2020. Interferon-induced transmembrane protein 3 genetic variant rs12252-C associated with disease severity in coronavirus disease 2019. J. Infect. Dis. 222, 34–37.
Zhao, X., Guo, F., Liu, F., Cuconati, A., Chang, J., Block, T., Guo, J., 2014. Interferon induction of IFITM proteins promotes infection by human coronavirus OC43. Proc. Natl. Acad. Sci. U. S. A. 111, 6756–6761.